NEUTRON QUASI-ELASTIC SCATTERING STUDY OF ROTATIONAL MOTIONS IN THE SMECTIC C, H AND VI PHASES OF TEREPHTAL-BIS-BUTYL-ANILINE (TBBA)

F. Volino, A. Dianoux, H. Hervet

NEUTRON QUASI-ELASTIC SCATTERING STUDY OF ROTATIONAL MOTIONS IN THE SMECTIC C, H AND VI PHASES OF TEREPHTAL-BIS-BUTYL-ANILINE (TBBA)

F. VOLINO

Institut Max von Laue-Paul Langevin, 156 X, 38042 Grenoble Cedex, France

and

Groupe de Dynamique des Phases Condensées, Laboratoire de Cristallographie (*)
Université des Sciences et Techniques du Languedoc,
place Eugène-Bataillon, 34060 Montpellier, France

and

A. J. DIANOUX

Institut Max von Laue-Paul Langevin, 156 X, 38042 Grenoble Cedex, France

and

H. HERVET

Collège de France, Laboratoire de Physique de la Matière Condensée,
place Marcelin Berthelot, 75231 Paris, Cedex 05, France

Résumé. — On présente une étude des mouvements rotationnels dans les phases smectiques C, H et VI du TBBA, par diffusion quasi élastique, incohérente, de neutrons (NQES). Les spectres expérimentaux sont analysés à l'aide du facteur de structure élastique incohérent (EISF). Pour interpréter sa variation en fonction du moment de transfert neutronique et de la température, on a raffiné le modèle de rotation uniaxiale utilisé précédemment [2] en incluant des fluctuations additionnelles, rapides (échelle de temps : 10^{-11} s) du grand axe du corps de la molécule. On considère ici les vraies valeurs (plutôt qu'une valeur moyenne) des rayons de gyration autour de cet axe, des différents protons. On trouve qu'un tel modèle décrit de manière satisfaisante les données pour toutes les températures entre 152 °C (SmC) et 94 °C (SmH surfondue). Le paramètre d'ordre de l'axe du corps, défini par $S_1 = < \cos \lambda >$ où λ représente l'écart par rapport à la position moyenne, varie de 0,5-0,6 à 152 °C à 0,95 à 94 °C. Le temps de corrélation du mouvement varie de 1 à 3 $\times$ 10^{-11} s dans ce même intervalle de température. A la transition SmH-SmVI, il y a arrêt complet (toujours par rapport à la même échelle de temps) des fluctuations de cet axe et apparition d'un ordre orientationnel pour la rotation autour de cet axe. On discute l'influence sur cette analyse de possibles (rapides) isomérisations du corps. On montre aussi que l'histoire thermique de l'échantillon est un facteur important pour obtenir des résultats reproductibles. Enfin le calcul de l'EISF de quelques modèles discutés dans le texte est présenté dans l'Appendice.

Abstract. — A study of rotational motions in the smectic C, H and VI phases of TBBA by means of incoherent neutron quasi-elastic scattering (NQES) is presented. The data are analyzed in terms of the elastic incoherent structure factor (EISF). To interpret its dependence versus neutron momentum transfer and temperature, the simple, uniaxial rotational model used in previous work [2] is refined by including additional, rapid (time scale : 10^{-11} s) fluctuations of the body long axis. The true gyration radii (rather than an average value) of the various protons are now considered. It is found that this model describes satisfactorily the data for all temperatures between 152 °C (Sm C) and 94°C (supercooled SmH). The order parameter, defined by $S_1 = < \cos \lambda >$, characterizing the axis fluctuations, is found to vary from 0.5-0.6 at 152 °C to $\approx$ 0.95 at 94 °C. The average reorientational correlation time changes from about 1 to 3 $\times$ 10^{-11} s in this temperature range. At the SmH-SmVI transition, there is complete quenching (on the same time scale) of these fluctuations and the onset of orientational ordering around this axis. The possible influence on this analysis of the body isomerisation is discussed. The thermal history of the sample is shown to be an important factor for obtaining reproducible results. The calculation of the EISF of various rotational models discussed is also presented.

(*) Laboratoire associé au C. N. R. S.

1. **Introduction.** — The study of random molecular motions in liquid crystalline terephtal-bis-butyl-aniline (TBBA) by neutron quasi-elastic scattering (NQES) using the partial deuteration method has led, up to now, to the following results :

(i) in the solid phase, the body rotation is quenched or rather slow ($\tau_R > 10^{-10}$ s), but the extremities of the butyl chains (probably the last methylene and methyl groups) reorient rapidly ($\tau_R \approx 10^{-11}$ s) [1] ;

(ii) in the smectic H phase at 119 °C, the data could be interpreted in terms of a rapid ($\tau_R \approx 1.5 \times 10^{-11}$ s) uniaxial rotational diffusion of the molecules around their long axis [2]. Later, it was shown [3] that these data were inconsistent with the idea of an orientational ordering of the molecules around this axis, as foreseen by the Meyer-McMillan microscopic theory [4]. In the whole SmH phase, the self diffusion coefficient was found to be smaller than 6×10^{-8} cm^2/s [5] ;

(iii) on the contrary, when the sample was cooled rapidly (in one or two minutes) from 130 °C (SmH phase) to 88 °C, near the temperature where supercooled SmH-SmVI phase transition should occur, the data could be analysed in terms of a model implying such a partial orientational ordering [6]. It was suggeste that this phenomenon could be a pretransitional effect to the SmH-SmVI transition ;

(iv) finally, in the smectic C and A phases, the translational motions were found to be rather rapid, leading to average self-diffusion coefficients of 1 to 3×10^{-6} cm^2/s [5, 7].

In this paper, we present a more detailed NQES study of the rotational motions in the SmC, SmH and SmVI phases of TBBA. In section 2, we describe the experimental conditions, the neutron spectra and the way in which they are handled. In section 3, we analyse the data in terms of the elastic incoherent structure factor (EISF) and rotational correlation times. These results are discussed in section 4. In the Appendix, we present the calculation of the EISF of the various models discussed in the data analysis.

2. **Experimental.** — 2.1 THE DTBBA MOLECULE — The sample studied was the partially deuterated specimen of TBBA which we called DTBBA in previous works [1, 6]. The molecule is schematized in its trans conformation in figure 1. The straight line passing through the centers of the three phenyl rings can be defined as the molecular axis (in fact, the body axis). This axis makes an angle of about 10° with the para-axes of the rings [8]. Assuming that the body is rigid and can reorient around this axis, the gyration radii a_i of the various protons can be calculated exactly. These are listed in table I together with the distances R_i of these protons to the center of symmetry of the molecule. Because of this symmetry, only half of the molecule will be considered in the following. If the body isomerisation is included in the motion, some of these radii must be replaced by an average value, and the axes of the corresponding average circles allowed to precess on a cone of apex angle $\approx 20°$. This last point is discussed in the Appendix. The contribution to the total intensity of the nuclei other than the 10 protons of the molecule (mainly the 22 deuterons) is about 5 %. Since this intensity is not concentrated around $\omega = 0$ but rather spread out over all the spectra (the chains move at least as rapidly as the body), it will not change appreciably the shape of the proton spectra and will be neglected in the following.

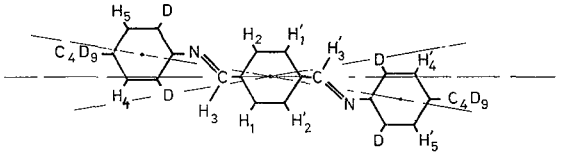

FIG. 1. — Sketch of the DTBBA molecule in its trans-conformation. Assuming a rigid body, there are five kinds of different protons labelled from 1 to 5. The new body axis after a trans-trans isomerisation is also shown.

TABLE I

Gyration radii of the protons of the DTBBA molecule. See fig. 1 and 6

Protons	H_1, H'_1	H_2, H'_2	H_3, H'_3	H_4, H'_4	H_5, H'_5
a_i (Å)	2.33	1.90	1.52	2.33	1.90
R_i (Å)	2.48	2.48	3.60	7.60	8.15

2.2 NEUTRON SCATTERING. — The neutron spectra were obtained with the time-of-flight multichopper spectrometer IN5, installed at the cold source of the Institute Laue-Langevin. The incident wavelengths used were 8.25 and 9.48 Å yielding elastic resolutions

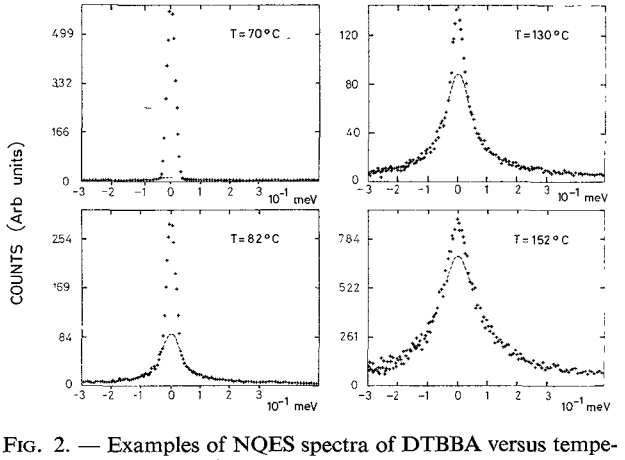

FIG. 2. — Examples of NQES spectra of DTBBA versus temperature for $Q = 0.92$ Å^{-1}. The separation between elastic and quasi-elastic line is shown by a dotted line. The number of counts have been normalized so that it makes sense to compare the amplitudes of the four spectra. Incident wavelength 9.48 Å.

$\Delta\omega$ of 40 and 33 μeV FWHM respectively. The container and temperature regulation systems were the same as in previous work [1, 2, 5, 6]. Two kinds of runs were performed. First, many angles were recorded simultaneously for elastic neutron momentum transfers Q ranging between 0.2 and 1.4 $Å^{-1}$. The temperatures were 137 °C (SmH) and 151 °C (SmC). The idea here was to obtain detailed information on the geometry of the motions. In the second kind of runs all the detectors were gathered around two angles, corresponding to average Q values of 0.92 and 1.18 $Å^{-1}$. The idea here was to study the temperature variation of the motions. In all cases, the NQES spectra were similar to those already published [2], namely they were composed of a narrow elastic peak (width of the resolution function) superimposed on a broadened line (quasi-elastic peak), a behaviour which is characteristic of a random rotational motion. Examples of spectra are shown in figure 1.

2.3 DATA ANALYSIS. — In a first stage, we tried to analyse the neutron spectra in terms of the uniaxial rotational model used previously for 119 °C [2]. However it turned out rapidly that such a model was now insufficient to describe the higher temperature data, especially at high Q values ($\approx$ 1.2 $Å^{-1}$), by predicting an elastic intensity definitely greater than observed. This observation indicates that the motion is more *isotropic* than allowed by the uniaxial model. The only way to make the motion more isotropic is to allow the molecular axis (in fact the body axis) to fluctuate about its equilibrium position, on a time scale of a few 10^{-11} s. The superposition of reorientation around the long axis and fluctuation of this axis is certainly not easy to describe with a rate equation of the kind used in similar problems [9]. However, whatever the details of this motion, the scattering law, in the quasi-elastic region, is necessarily of the form

$$S(Q, \omega) = B_0(Q)\,\delta(\omega) + \frac{1}{\pi}\sum_n B_n(Q)\,L_n(\omega)\,. \quad (1)$$

In this expression, $B_0(Q)$ is the EISF of the rotational model, $B_n(Q)$ are coefficients and $L_n(\omega)$ are Lorentzian depending on one or a few characteristic times.

Moreover, it verifies the following sum rule :

$$\int S(Q, \omega)\,d\omega = 1 \quad (2a)$$

which in case of eq. (1) reduces to :

$$B_0(Q) + \sum_n B_n(Q) = 1\,. \quad (2b)$$

It is seen that the EISF is the fraction of the total (quasi-elastic) intensity, which is contained in the purely elastic term. This property can be used to extract its experimental value. When the elastic and quasi-elastic contributions are well separated, the separation is completed by natural extrapolation and the two contributions are measured by graphical integration. This procedure was used in the previous work, and gives satisfactory results when the wings of the spectra are not too important. In the opposite case, the uncertainty in the determination of the total intensity (due mainly to the uncertainty in the background level) makes this determination less precise, so that another method (namely a computer method) is required. In this method, a normalized scattering function such as eq. (1) is fitted to each experimental spectrum. The number of parameters is chosen to be small (3 or 4) and the best value found for $B_0(Q)$ is the experimental EISF. The mathematical form of the sum in the right hand side of eq. (1) should be chosen such that it approximates in the best manner the broadened quasi-elastic line. We considered two cases :

(i) the broadened component is approximated by a single lorentzian. This approximation seems reasonnable when observing the experimental spectra. The scattering law is thus :

$$S_1(Q, \omega) = b\delta(\omega) + \frac{1}{\pi}(1 - b)\frac{\tau}{1 + \omega^2\tau^2}\,. \quad (3)$$

The parameters are b, τ and a constant background. The fitting procedure is described in reference [1]. The result is that the values of the EISF b are practically identical to those obtained by graphical integration when this method is applicable ;

(ii) the scattering law is approximated by the following function :

$$S_2(Q, \omega) = pA_0(Q)\,\delta(\omega) + \frac{1}{\pi}[A_1(Q) + (1 - p)\,A_0(Q)]\,L_1(\omega) + \frac{1}{\pi}\sum_{n=2}^{N} A_n(Q)\,L_n(\omega) \quad (4)$$

where the expressions of $A_n(Q)$ and $L_n(\omega)$ are those of the uniaxial rotational model used previously [2, 9]. It is seen that eq. (4) is a modified uniaxial scattering law (not modified if $p = 1$), in which we have transferred the excess or lack of intensity of the elastic line into the first Lorentzian. The parameters are p, the HWHM : $1/\tau_1$ of the first Lorentzian, a gyration radius a, and a constant background. The choice of a scattering law such as eq. (4) is justified in our case since the uniaxial rotational motion around the long axis is the main phenomenon responsible for the neutron spectra. It turned out that starting from different but reasonable values of the parameters, the result of the fit was stable. For spectra where the elastic amplitude is small, the values of the EISF using eq. (4) or eq. (3) are found to be practically the same. When the elastic amplitude is greater eq. (4) yields a value of the EISF systematically smaller than eq. (3). This can be understood since eq. (4) emphasizes more than eq. (3) what occurs in the wings of the spectra. The most reliable experimental value lies probably between these two values.

3. **Results.** — 3.1 GEOMETRY OF THE MOTION. — Figure 3 shows the experimental EISF versus Q for 137 °C (SmH) and 151 °C (SmC). The data for 119 °C (SmH) obtained from previous work [2] are also

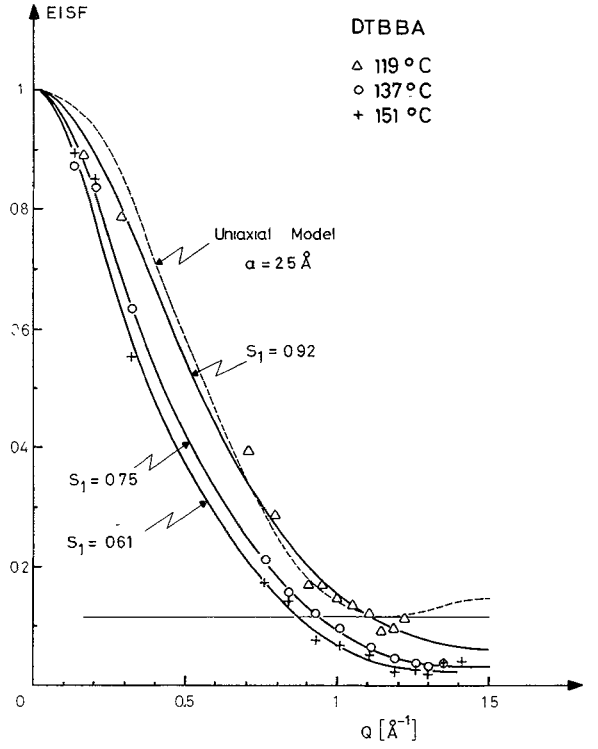

FIG. 3. — Experimental EISF as a function of Q for DTBBA for various temperatures. △ : 119 °C (SmH), ○ : 137 °C (SmH), + : 151 °C (SmC). The data at 119 °C are the same as those of reference [2]. The full curves are theoretical curves representing eq. (7) for various values of the order parameter S_1. The dashed curve is the theoretical fit of the uniaxial model used in reference [2], to the data at 119 °C. The theoretical minimum value ($\approx$ 0.11) of the EISF for a purely uniaxial model is also shown. The experimental values of the EISF were obtained by fitting eq. (4) to the experimental spectra, as explained in the text.

shown for comparison. The theoretical minimum value ($\approx$ 0.11) for a purely uniaxial rotational motion is indicated. As mentioned before the data for 137 and 151 °C above 1 Å^{-1} fall well below this value indicating an additional motion of the molecular axis. Models taking into account such additional motion are presented in the Appendix and the corresponding EISF are calculated. The most important points concerning this axis motion are the following :

(i) although the molecule is symmetric (change of the polar angle λ into $\lambda + \pi$ does not change the geometry), it is necessary here to choose an angular distribution function for the molecular axis which is peaked at only *one* point in space. The reason for this is that the EISF is a quantity which pictures the various positions of the protons after a time of the order of $10(\Delta\omega)^{-1}$ (a few 10^{-10} s in the present case). The choice of a distribution peaked at 0 and π would mean that the molecule is able to flip by an angle π during this time, which is certainly not reasonable ;

(ii) λ and φ being the polar and azimuthal angles of the molecular (body) axis, and assuming a distribution function $p(\lambda, \varphi) = f(\lambda).g(\varphi)$ the most natural definitions for order parameters for the molecular axis are the average of cos λ and cos φ rather than the average value of $\frac{1}{2}$ (3 cos^2 λ − 1), which is relevant for analysis of NMR data ;

(iii) in the Appendix, two models are presented. We will restrict ourselves here to model 1 which assumes $g(\varphi)$ = Cte. The reason is that this is a *one* parameter model which, as we shall see, is sufficient to describe the data. It assumes that the body axis can fluctuate around its equilibrium position (the director), according to the (normalized) law :

$$f(\lambda) = \frac{\delta'}{2 \operatorname{sh} \delta'} e^{\delta' \cos \lambda}. \tag{5}$$

The order parameter $S_1 = < \cos \lambda >$ is related to the parameter δ' by

$$S_1 = \coth \delta' - \frac{1}{\delta'} \tag{6}$$

and the expression of the EISF to be used for comparison with the data of figure 1 should be an average over the five kinds of different protons of the DTBBA molecule, of eq. (A.23), namely :

$$\overline{A_0(Q)} = \frac{1}{5} \sum_{i=1}^{5} \sum_{l=0}^{\infty} (2l + 1) j_l^2(QR_i) S_l^2(\delta') P_l^2(\cos \mu_i) \tag{7}$$

where the a_i and R_i are given in table I and

$$\sin \mu_i = \frac{a_i}{R_i}. \tag{8}$$

The full lines in figure 3 are theoretical curves representing eq. (7) for a few values of δ' (or S_1). It is seen that they reproduce quite satisfactorily the data for 151, 137 and 119 °C with values for S_1 around 0.6, 0.75 and 0.9, respectively. The fact that this one parameter model reproduces well the Q dependence of the EISF is a good support for its validity.

At this point it is interesting to compare the fit of the data at 119 °C by the present model and by that one used in the former papers [2, 3]. In broken line is represented the best fit of the uniaxial model used previously. It is seen that due to the lack of experimental points above 1.2 Å^{-1} and to the relatively high value of S_1 ($\approx$ 0.9) the two descriptions are roughly equivalent. In other words, in this case, the fluctuation of the body axis is roughly equivalent to an increase of the average gyration radius from about 2.0 to 2.5 Å.

3.2 VARIATION WITH TEMPERATURE. — Figure 4 represents the variation of the EISF measured at

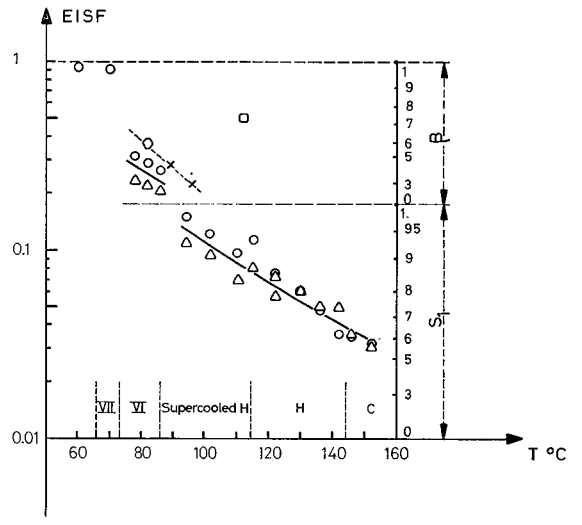

FIG. 4. — Experimental EISF of DTBBA, for $Q = 1.18$ Å^{-1}, as a function of temperature. △, ○ : from spectra obtained by cooling gently the sample steps by steps. △ : value obtained using eq. (4), ○ : value obtained using eq. (3). ⟨◯⟩, ×, △ : from spectra obtained after rapid cooling, as explained in the text ; ⟨◯⟩ and □ : average of values obtained using eq. (3) and (4), × : interpolated from figure 2 of reference [6]. The transition temperature determined by differential thermal analysis (on this partially deuterated specimen) are also shown. On the right part of the graph are represented the corresponding scales yielding the values of the two order parameters defined in the text : $S_1 = < \cos \lambda >$ order parameter for the body axis fluctuations ; $\beta = < \cos \varphi' >$ order parameter for orientational ordering around the body axis. The data for $Q = 0.92$ Å^{-1} are not represented, for clarity, but yield a very similar variation.

$Q = 1.18$ Å^{-1} as a function of temperature. This Q value was chosen since it corresponds to a point (near the minimum) where $\overline{A_0(Q)}$ is the most sensitive to the details of the rotational model. It is seen that the EISF smoothly increases from 152 °C in the SmC phase to 94 °C into the supercooled SmH phase without any significant discontinuity at 144 °C (SmH-SmC) or at 114 °C (solid-SmH). On the contrary, it apparently, suffers a definite jump between 94 °C and 86 °C temperature range where the SmH-SmVI transition should occur. Between 86 and 78 °C (in principle in the VI phase) it again changes smoothly, and below 77 °C (SmVII phase ?) it suffers a more drastic jump (the intensity is almost purely elastic). Let us analyse these results in terms of order parameters. Consider eqs. (6) and (7). For fixed Q, at each value of A_0 corresponds one value of $S_1 = < \cos \lambda >$. Such a correspondence is shown on the right-hand vertical scale on figure 4 for $Q = 1.18$ Å^{-1}. It is seen that S_1 increases smoothly from 0.5-0.6 at 152 °C to about 0.95 at 94 °C and that the SmH-SmVI transition can be considered as a quenching of the axis fluctuations. In the VI phase, the pure uniaxial model ($S_1 = 1$) is even not sufficient to explain the data so that an orientational ordering around the long molecular axis can be invoked, as in reference [6]. Similarly as above, combining (A.32) and (A.7), for fixed Q, at each value of A_0 corresponds a value of $\beta = < \cos \varphi' >$, the order parameter around the long axis. Such a scale is also indicated in figure 4. It is seen that the VI phase corresponds to $< \cos \varphi' > \approx 0.3$-$0.5$. Finally, below 77 °C (SmVII phase ?), the quasi-elastic intensity is very small (of the same order of magnitude than in the solid phase [1]). This means that, either the orientational ordering is much greater or the time scale of the motion is much longer. Probably both reasons combine. Only an experiment at much higher energy resolution can give a definite conclusion.

3.3 CORRELATION TIMES. — Figure 5 represents τ_1 as a function of temperature, where $1/\tau_1$ is the HWHM of the first Lorentzian line of eq. (4). For a pure uniaxial model, $1/\tau_1$ is the rotational diffusion coefficient [9]. For the present case of a more complex motion, it is also reasonable to give it the same physical meaning since in the first approximation, the rotation around the long axis is the main contribution to the NQES spectra. It is seen that the Arrhenius plot shows no discontinuity of τ_1 through all the phases, and that the deduced *activation energy* of about 3.8 kcal/mole is of a good order of magnitude for a rotational motion in a molecular system.

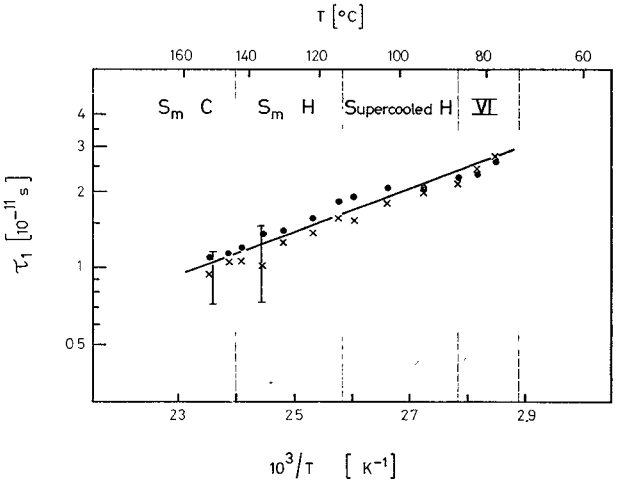

FIG. 5. — Average orientational correlation times of DTBBA versus reciprocal temperature, X, ● : from spectra obtained at $Q = 1.18$ Å^{-1} and $Q = 0.92$ Å^{-1}, respectively ; ⟊ : spread of the values determined from 13 spectra, with Q varying between 0.2 and 1.4 Å^{-1} at 137 and 151 °C. The slope of this *Arrhenius plot* is about 3.8 kcal/mole.

4. **Discussion.** — 4.1 SUMMARY OF THE RESULTS. — At the present stage of the analysis, it can be said that, assuming that the body of the molecule of TBBA is rigid in its trans conformation, during a time of a few 10^{-10} s, the body motion can be described by the superposition of a rotational diffusion around its long axis, plus fluctuation of this axis around its equilibrium orientation. This fluctuation is characterized by an order parameter $S_1 = < \cos \lambda >$, which is

rather small in the C phase ($S_1 \approx 0.5$-0.6 at 152 °C), and increases steadily as the SmH-SmVI transition temperature is approached. At the transition this fluctuation is quenched (always on the same time scale) and orientational ordering around the long axis appears. The correlation time of these motions varies from 1 to 3 $\times$ 10^{-11} s in the whole temperature range studied.

4.2 BODY ISOMERISATION. — So far, we have considered that the body is rigid. However, as pointed out by some authors [10], one possible motion of the molecules is the trans-trans isomerisation through the cis-conformation. This isomerism has been invoked to explain the magnetic equivalence of the four deuterons on each phenyl ring of the corresponding deuterated TBBA specimens [10]. Is this motion relevant for our analysis ? Probably not for the following reasons :

(i) general considerations on inertia momenta and energy barriers show that if the isomerism is possible on a time scale of say 10^{-7} s (the NMR time scale) it is highly improbable during a few 10^{-10} s (the neutron time scale), and that during this time, the body only rotates in its most probable (i. e. trans) conformation ;

(ii) let us assume however that this isomerisation could happen frequently in 10^{-10} s. In this case, as explained in the Appendix, this could be taken into account in the expression of the EISF by merely multiplying the right hand side of eq. (7) by $P_l^2(\cos \nu)$ where ν ($\approx 10°$) is the angle between the body axis in the trans and the cis-conformations. Calculating this, we have verified that, due to the relatively small value of ν, the EISF is practically unchanged. Consequently, the isomerisation of the molecules, although highly improbable on the neutron time scale is in any case practically irrelevant for the analysis of these neutron data.

4.3 INTERPRETATION OF THE VALUE OF THE ORDER PARAMETERS. — The value $S_1 \approx 0.5$-0.6 for the fluctuations of the body axis in the C phase is in fact rather small since it corresponds, within the framework of model 1, to fluctuations of $\pm$ 50 to 60° around the average position (director). Does this mean that the (low energy) fluctuations within the smectic planes (at constant tilt angle) have the same probability than the (higher energy) fluctuations out or inside the planes ? Probably not, and model 2 developed in the Appendix, which takes into account this difference, would have been more *realistic* to interpret the data. We did not use it however, since it is a three parameter model whereas the one we used depends only on one. The accuracy of the data would have probably led to a non unique determination of these parameters except if some hypothesis on their values is made. In this sense, it would not have brought more information than model 1. However, we think that the estimated S_1 values should be interpreted as an average of the two kinds of fluctuations mentioned. This point is supported by the following considerations. From the value of S_1, one can estimate the order parameter S_2' that would be deduced from a NMR experiment, for example from the dipolar splitting of two protons in a phenyl ring. Within the framework of model 1, a fluctuation of $\pm$ 50 to 60° of the body axis would correspond to values of $S_2' = \frac{1}{2} < 3 \cos^2 \lambda - 1 >$ between 0.3 and 0.4 (the average $< >$ is performed using a Maier-Saupe distribution). These values do not seem very reasonable since they are smaller than what is found for nematics. On the contrary, with a model such model 3, it is possible to imagine motions which permit larger azimuthal than polar fluctuations, leading to higher values of S_2'.

In the SmH phase, the amplitude (but not the time scale) of these fluctuations is found to decrease with temperature to a very small value at the H-VI transition. However, more detailed experimental results are needed to determine how these fluctuations are quenched at the SmH-SmVI transition.

For the orientational ordering in the SmVI phase, the break of symmetry from pseudo-hexagonal to pseudo-orthorhombic lattice [12] makes the uniform rotation around the body axis less probable. The molecules tend now to orient their phenyl rings towards fixed directions in space, corresponding to the herringbone arrangement [11, 12] with no possibility in a few 10^{-10} s to flip by π around this axis. However, large amplitude, but overdamped oscillations on this time scale can occur around these equilibrium positions, which appear in the neutron spectra as quasi-elastic scattering. The value of the orientational parameter $\beta = < \cos \varphi' >$ reflects the amplitude of these oscillations. The above picture is consistent with the X-ray data [11] which show a fixed direction in space for the molecules, but intense diffuse scattering.

In all cases, what is remarkable is the time scale of the motions. In particular the finding that the body (thus the molecular axis) fluctuates so rapidly seems surprising. However, similar rapid axis fluctuations have been invoked to explain spin-lattice relaxation results in nematic PAA [21].

4.4 INFLUENCE OF THE THERMAL HISTORY OF THE SAMPLE. — Consider figure 4. Apart from the data already discussed (triangles and circles) which were extracted from neutron spectra, obtained as the sample was cooled down by steps of a few degrees, there are three other points namely the hexagon, crosses and square which apparently do not fit within the above picture. The hexagon was obtained, when after heating the sample to 130 °C in the H phase during 15 mn, it was cooled rapidly (in about 1 mn) to 82 °C, and the spectra recorded during about two hours. The crosses correspond to about the same thermal history, but data were recorded during about 24 h, using another incident wavelength, and another sample. In fact, they correspond to the data of reference [6]. Finally, the most strange point is the square : the

sample was first prepared by heating it to about 150 °C in the SmC phase, then cooled down rapidly to room temperature where it stayed about 24 h. Then it was heated to 111 °C, four degrees below the normal solid-SmH transition temperature and the spectra recorded. These three different results suggest the following remarks :

(i) to obtain reliable results, one must be careful in the way in which the temperature of the sample is reached ;

(ii) if the cooling is too rapid, one probably misses the « normal » metastable phases, and obtains other metastable phases, which can be thought of as *quenched* smectic H phases (hexagon and cross) or quenched smectic C phase (square). This last case is significant. When quenched from the SmC to room temperature, the molecules could not rearrange themselves in order to make the crystalline array. Rather, some kind of amorphous state is reached, where the molecules are somewhat disordered. When the sample is heated near the Solid-SmH temperature, the molecules, which have probably more space than in the crystal, can perform large and rapid fluctuations around their equilibrium position. This is not possible in the well packed crystalline phase. When finally the temperature is increased from this state to 115 °C, one degree above the solid-SmH transition temperature, some time is probably needed to obtain the true H phase, starting from this strange state. This may explain why the points at 115 °C in figure 4 are slightly outside the average curve ;

(iii) as a consequence of this, what was observed in reference [6] was certainly orientational ordering of the molecules, but the fact that it corresponds to a pretransitional effect might be questioned.

5. **Conclusions.** — The conclusions which should be drawn from the present work are, in our opinion, of two kinds : the first concerns the physics and the second the experimental technique used.

For the physics, we have shown that in the smectic VI, H and C phases, as far as the body motions of the TBBA are concerned, these are very rapid, with correlation times ($\approx 10^{-11}$ s), of the order of what can be expected in ordinary molecular liquids of similar molecular weights. The geometry of the motion is found to be more *isotropic* than generally expected.

In the VI phase where the body rotation is usually thought of as quenched [11, 12], we find that it can perform large amplitude, overdamped oscillations about its equilibrium position. In the H phase, which is usually considered a *plastic crystal* [11, 13], where the molecules rotate around their long axes, it is found that in addition, the body axes are rapidly jiggling around their equilibrium positions. The amplitudes of these oscillations become very large ($\approx$ 50-60°) in the C phase, and this may explain why a crystalline order can no more be maintained in the planes. Incidently we think that this axis motion should be taken into account for the interpretation of the shape of the NMR spectra, at least in the C and H phases. In our opinion, the decrease of the amplitude of these rapid fluctuations plays a major role in the broadening of the components of the NMR spectra. This role is probably greater than the slowing down of the rotation around the long axis, which, we have seen, is always very rapid ($\approx 10^{-11}$ s). [For NMR work on TBBA, see ref. [8, 10, 14-17]]. Data at higher temperatures are now needed to see how the complete isotropy of the motion is reached through the C, A, nematic and isotropic phases. For the chain motions, they are probably more rapid and isotropic than those of the body. This point has been verified qualitatively at 119 °C in the SmH phase [2].

For the experimental technique, the most important point has been to show the power of NQES at high resolution to obtain rather precise information on the geometry and the time scale of the molecular motions. This property is now well accepted and has been proved in more simple systems such as methyl group rotation [18]. However, this information is accurate on the reduced space and time scales defined by the available Q range — typically 0.2 to 2 $Å^{-1}$ — and frequency range — typically 10^{+10} to 10^{+12} rd/s. The Q range corresponds exactly to molecular distances — 30 to 3 Å —, but the frequency range to a rather narrow time window 10^{-10} to 10^{-12} s. In a given experiment, this window is even narrower. This limitation is in fact an advantage rather than an inconvenience since it allows a sampling of the motions at characteristic frequencies around $\Delta\omega$. All much slower motions are included in the elastic line, and considered as static, and much faster motions are considered as contributing in the inelastic spectrum. This observation shows that great care must be taken in interpreting the *experimental* values of the EISF. It is a quantity which depends not only on the physics, but also on the experimental window. Surprisingly however it is this property which makes it very useful for the study of the geometry of molecular motions.

Acknowledgments. — We are indebted to Prof. P. G. de Gennes, Drs. O. Parodi, B. Cabannes, J. Charvolin, B. Deloche and R. E. Lechner for very fruitful discussions regarding the results of this work. One of us (F. V.) wishes to express his gratitude to Dr. B. Bergwall for his interest during the preparation of the manuscript.

APPENDIX

In this Appendix, we calculate the elastic incoherent structure factor (EISF) for the models mentioned in the text. The motion is pictured as follows : the (incoherent) scattering center P can move on a circle

of radius a centered on O'. The axis Om of this circle can rotate around some origin O, the distance OO' being constant. Figure 6 summarizes the various

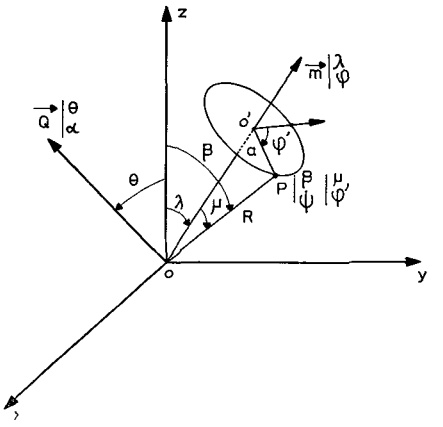

FIG. 6.

symbols used. The polar and azimuthal angles of the various vectors, with respect to some laboratory frame Oxyz are :

Om : λ and φ

OP : β and ψ

Q : θ and α

Let μ and φ' be the polar and azimuthal angles of **OP** with respect to a frame whose polar axis is **Om**. We have the relation

$$Y_l^m(\beta, \psi) = \sum_{n=-l}^{+l} D_{mn}^{l*}(\lambda, \varphi, ...)\ Y_l^n(\mu, \varphi') \quad (A.1)$$

where the Y_l^m are the spherical harmonics and D_{mn}^l the matrix elements of the irreducible representations of the full rotation group (Wigner matrices).

The EISF of the motion of P can be expressed as

$$\mathbf{A}_0(\mathbf{Q}) = < e^{i\mathbf{Q}.\mathbf{R}(t=\infty)}.e^{-i\mathbf{Q}.\mathbf{R}(t=0)} > \quad (A.2)$$

where the brackets indicate an average over all the possible initial and final positions of the scattering center. Since these two distributions are identical (ergodic theorem) eq. (A.2) reduces to

$$A_0(\mathbf{Q}) = | < e^{i\mathbf{Q}.\mathbf{R}} > |^2 . \quad (A.3)$$

We have considered the following distribution functions :

(i) distribution $p(\varphi')$ of P on the circle of radius a. In the case of uniform rotational motion, all the points are equivalent so that we can choose

$$p_1(\varphi') = \frac{1}{2\pi} . \quad (A.4)$$

If the motion is restricted to a jump motion among N equidistant sites $\mathbf{r}_j$ on the circle, one should rather choose the distribution

$$p_2(\varphi') = \frac{1}{N} \sum_{j=1}^{N} \delta(\mathbf{r} - \mathbf{r}_j) \quad (A.5)$$

$p_2(\varphi') \to p_1(\varphi')$ when $N \to \infty$. Such a distribution corresponds to the model used in reference [2].

If the points are not equally weighted as in the case of an orientational ordering around the body axis, one should rather take a peaked distribution. We then choose the (normalized) function [3, 6]

$$p_3(\varphi') = \frac{1}{2\pi I_0(\beta')} e^{\beta' \cos \varphi'} \quad (A.6)$$

where I_0 is the modified Bessel function of first kind of order 0. In this case, the orientational order parameter β is given by

$$\beta = < \cos \varphi' > = \frac{I_1(\beta')}{I_0(\beta')} , \quad (A.7)$$

(ii) distribution $q(\lambda, \varphi)$ of the body axis **Om** around the origin O (center of symmetry of the molecule). The approximation we shall always make is that the azimuthal (φ) and polar (λ) motions are independent, so that we can write

$$q(\lambda, \varphi) = f(\lambda)\, g(\varphi) . \quad (A.8)$$

The mathematical expressions of f and g will depend on the very problem. Suppose we are in a tilted smectic phase. There are two natural z axes : the direction of the director **d**, and the direction of the normal **n** to the smectic planes. The tilt angle ω is the angle between **n** and **d**. The most simple model is the one which ignores the smectic planes. The director **d** is taken as z axis, the distribution g will be chosen as constant

$$g(\varphi) = g_1(\varphi) = \frac{1}{2\pi} . \quad (A.9)$$

For the distribution f, peaked at $\lambda = 0$, we choose the following (normalized) function

$$f(\lambda) = f_1(\lambda) = \frac{\delta'}{2 \operatorname{sh} \delta'} e^{\delta' \cos \lambda} . \quad (A.10)$$

This model is simple because it depends only on one parameter δ', but ignores the fact that the molecules can fluctuate more easily in the smectic planes (at constant tilt angle), than out or inside the planes. To take this into account, one should choose **Oz** along **n**. The distributions to be taken are now :

$$g(\varphi) = g_2(\varphi) = \frac{1}{2\pi I_0(\gamma')} e^{\gamma' \cos \varphi} \quad (A.11)$$

and

$$f(\lambda) = f_2(\lambda) = A_2 . e^{\delta' \cos (\lambda - \lambda_m)} \quad (A.12)$$

with

$$A_2^{-1} = \int_0^{\pi} e^{\delta' \cos(\lambda - \lambda_m)} \sin \lambda \, d\lambda \,. \quad (A.13)$$

The azimuthal distribution is peaked at $\varphi = 0$, along the **C**-director (taken as **Ox** axis) and the polar distribution is peaked at some angle λ_m (which can be near, but not necessarily equal to the tilt angle ω). This model is more complicated than the former since it depends on the three parameters γ', δ' and λ_m. It simplifies in a smectic A phase since, in this case, we should have $\gamma' = 0$.

The expression of the EISF can now be easily calculated for various models.

MODEL 1. — Uniform rotation on the circle of radius a, plus fluctuation around the director. For the various averages, we should use eqs. (A.4), (A.9) and (A.10). We can write :

$$e^{i\mathbf{Q}.\mathbf{R}} = 4\pi \sum_{l=0}^{\infty} \sum_{m=-l}^{+l} i^l j_l(QR) \, Y_l^{m*}(\theta, \alpha) \, Y_l^m(\beta, \psi) \,. \quad (A.14)$$

Plugging (A.1) into (A.14), performing the average over φ' using (A.4), and using the following relations :

$$Y_l^0(\mu, \varphi') = \left(\frac{2l+1}{4\pi}\right)^{1/2} P_l(\cos \mu) \quad (A.15)$$

and

$$D_{m0}^l(\lambda, \varphi, ...) = \left(\frac{4\pi}{2l+1}\right)^{1/2} Y_l^m(\lambda, \varphi) \quad (A.16)$$

where P_l is the Legendre polynomial of order l, we obtain

$$\langle e^{i\mathbf{Q}.\mathbf{R}} \rangle_{\varphi'} = 4\pi \sum_{l=0}^{\infty} \sum_{m=-l}^{+l} i^l j_l(QR) \times \times Y_l^{m*}(\theta, \alpha) \, Y_l^m(\lambda, \varphi) \, P_l(\cos \mu) \,. \quad (A.17)$$

Only the averages over φ and λ are left. The average over φ using A.9 leaves only the $m = 0$ term in the second member of (A.17), and further average over λ using (A.10) finally yields :

$$\langle e^{i\mathbf{Q}.\mathbf{R}} \rangle_{\varphi',\varphi,\lambda} = \sum_{l=0}^{\infty} [4\pi(2l+1)]^{1/2} \, i^l j_l(QR) \times \times Y_l^{0*}(\theta, \alpha) \, S_l(\delta') \, P_l(\cos \mu) \quad (A.18)$$

with

$$S_l(\delta') = \frac{1}{2} \frac{\delta'}{\operatorname{sh} \delta'} \int_0^{\pi} P_l(\cos \lambda) \, e^{\delta' \cos \lambda} \sin \lambda \, d\lambda \,. \quad (A.19)$$

The $S_l(\delta')$ can be defined as successive order parameters of the molecular body axis for model 1. It can be easily verified that we have

$$S_0 = 1 \quad (A.20)$$

$$S_1 = \coth \delta' - \frac{1}{\delta'} \,. \quad (A.21)$$

More generally, that they verify the recurrence relation

$$S_{l+1} = -\frac{2l+1}{\delta'} S_l + S_{l-1} \,. \quad (A.22)$$

To obtain the EISF of the model, according to (A.3), we must take the modulus squared of the second member of (A.18). In the case of a powder sample, the result is simpler. Averaging over all possible directions of **Q** and using the orthogonality properties of the Y_l^m, we finally get

$$\overline{A_0(Q)} = \sum_{l=0}^{\infty} (2l+1) \, j_l^2(Q.R) \, S_l^2(\delta') \, P_l^2(\cos \mu) \,. \quad (A.23)$$

From this expression, one should recover some limiting cases :

(i) the case $\delta' \to \infty$ corresponds to the uniform uniaxial motion on the circle of radius a. In this case, we have $S_l = 1$ and we can write

$$\overline{A_0(Q)} = \sum_{l=0}^{\infty} (2l+1) \, j_l^2\left(Q \frac{a}{\sin \mu}\right) P_l^2(\cos \mu) \,. \quad (A.24)$$

For physical reasons at least, this expression should be independent of μ and identical to eq. (2) of reference [2] for $N \to \infty$, namely

$$\overline{A_0(Q)} = \frac{1}{\pi} \int_0^{\pi} j_0(2 \, Qa \sin x) \, dx \,. \quad (A.25)$$

Although no direct mathematical demonstration could be found by us for these two properties, we have verified them numerically, to a high accuracy ;

(ii) in the case $\delta' = 0$, we have $S_l = \delta_{l0}$. Eq. (A.23) reduces to

$$\overline{A_0(Q)} = j_0^2(QR) \,. \quad (A.26)$$

This is the EISF of a sphere of radius R. Incidently this shows the various manners of generating this sphere with circles of radius a. The case with $a = 0$ corresponds to the so-called Sears expression ;

(iii) finally, the case $a = 0$ (thus $\cos \mu = 1$) corresponds to a motion on a sphere of radius R on which the distribution function is peaked at one point. We get :

$$\overline{A_0(Q)} = \sum_{l=0}^{\infty} (2l+1) \, j_l^2(QR) \, S_l^2(\delta') \,. \quad (A.27)$$

MODEL 2. — In this model we consider uniform rotation on the circle, plus fluctuation of the axis taking into account the existence of the smectic planes. The various average must be performed using (A.4), (A.11), (A.12). The same calculation than before holds until eq. (A.17), then one has to average over φ and λ using (A.11) and (A.12). For this purpose, it is

worth replacing the spherical harmonics by Legendre functions P_l^m defined by

$$Y_l^m(\lambda, \varphi) = (-1)^{|m|} \left[\frac{2l+1}{4\pi} \frac{(l-|m|)!}{(l+|m|)!}\right]^{1/2} \times \times P_l^{|m|}(\cos\lambda)\, e^{im\varphi} . \quad (A.28)$$

The average over φ using (A.11) yields :

$$< e^{\pm im\varphi} > = \frac{I_m(\gamma')}{I_0(\gamma')} \quad (A.29)$$

where I_m are the modified Bessel functions of first kind of order m. The average over λ using (A.12) leads to the introduction of other order parameters $F_l^m(\delta')$ defined by :

$$F_l^m(\delta') = A_2 \int_0^\pi P_l^m(\cos\lambda)\, e^{\delta' \cos(\lambda - \lambda_m)} \sin\lambda\, d\lambda . \quad (A.30)$$

Using all these expressions, it is straightforward but lengthy to write down the most general expression for the EISF. As before, in the case of a powder sample, the result is simpler, namely

$$\overline{A_0(Q)} = \sum_{l=0}^{\infty} (2l+1) j_l^2(QR) \times \times \left\{ F_l^0{}^2(\delta') + 2 \sum_{m=1}^{l} \frac{(l-m)!}{(l+m)!} F_l^m{}^2(\delta') \frac{I_m^2(\gamma')}{I_0^2(\gamma')} \right\} P_l^2(\cos\mu) . \quad (A.31)$$

For $\gamma' = 0$ and $\lambda_m = 0$, one recovers eq. (A.23). However, for $\gamma' = 0$ only, the results are different. This difference may be used to test smectic A models : molecules pictured either fluctuating around the normal to the smectic planes (uniaxial model) or fluctuating around some direction λ_m and rotating on a cone of apex angle $2\lambda_m$ (model proposed by Lösche *et al.* [19, 20]).

MODEL 3. — No fluctuation of the body axis, but orientational ordering on the circle of radius a.

In this case, rather than using the above formalism, it is worth using that of reference 3. The calculation is very similar except that we use here a continuous distribution rather than a discrete one. The result is

$$\overline{A_0(Q)} = \frac{1}{\pi I_0^2(\beta')} \int_0^\pi j_0(2\, Qa \sin x)\, I_0(2\, \beta' \cos x)\, dx . \quad (A.32)$$

MODEL 4. — This model corresponds to model 1 or 2 where in addition to the other motions the axis **Om** of the circle of radius a can precess on a cone of apex angle $2v$ around OO'. This motion roughly pictures the possibility for the body of the TBBA molecule to suffer trans-trans isomerisations through the (less stable) cis conformation. Indeed, consider figure 1. It is seen that the trans-trans isomerisation corresponds to an exchange of the following protons : $H_1 \rightarrow H_2$, $H_4 \rightarrow H_5$ and the same thing for the H' protons, plus a tilt of the body axis of about 2×10^o. In a frame attached to this axis, this motion is roughly equivalent to a tilt angle of 2×10^o of the axis of the average circle where are moving the exchanging protons.

The average circle can also be pictured as precessing on a cone of apex angle 2×10^o. This kind of motion can *a priori* be of importance for the analysis of the present data, since without any motion of the body axis, the protons motion is more *isotropic* than in the purely uniaxial model. This can be included in the calculation of the EISF. The details will not be given here, but the result is that the second members of eqs. (A.23) and (A.31) must be multiplied by $P_l^2(\cos v)$. It is seen that as far as v is small (in particular if $v \doteq 10^o$), the contribution of this factor is rather small.

References and footnote

[1] VOLINO, F., DIANOUX, A. J., LECHNER, R. E. and HERVET, H., *J. Physique Colloq.* **36** (1975) C 1-84.

[2] HERVET, H., VOLINO, F., DIANOUX, A. J. and LECHNER, R. E., *J. Physique Lett.* **35** (1974) L-151.

[3] HERVET, H., VOLINO, F., DIANOUX, A. J. and LECHNER, R. E., *Phys. Rev. Lett.* **34** (1975) 451.

[4] MEYER, R. J. and MCMILLAN, W. L., *Phys. Rev.* A **9** (1974) 899.

[5] DIANOUX, A. J., VOLINO, F., HEIDEMANN, A. and HERVET, H., *J. Phys. Lett.* **36** (1975) L-275.

[6] VOLINO, F., DIANOUX, A. J. and HERVET, H., *Solid State Commun.* **18** (1976) 453.

[7] These values of the self-diffusion coefficient, measured by NQES using the back scattering technique, turn out to be in excellent agreement with those determined recently by NMR : KRUGER, G. J., SPIESECKE, H. and STEENWINKEL, R., this conference.

[8] LUZ, Z., HEW, R. C. and MEIBOOM, H., *J. Chem. Phys.* **61** (1974) 1758.

[9] DIANOUX, A. J., VOLINO, F. and HERVET, H., *Mol. Phys.* **30** (1975) 1181.

[10] CHARVOLIN, J. and DELOCHE, B., *J. Physique Colloq.* **37** (1976) C 3-69.

[11] DOUCET, J., LEVELUT, A. M. and LAMBERT, M., *Phys. Rev. Lett.* **32** (1974) 301.

[12] DOUCET, J., LEVELUT, A. M., LAMBERT, M., LIEBERT, L. and STRZELECKI, L., *J. Physique Colloq.* **36** (1975) C 1-13.

[13] LEVELUT, A. M. and LAMBERT, M., *C. R. Hebd. Séan. Acad. Sci.* **272** (1971) 1018.

[14] DELOCHE, B., CHARVOLIN, J., LIEBERT, L. and STRZELECKI, L., *J. Physique Colloq.* **36** (1975) C 1-21.

[15] WISE, R. A., SMITH, D. H. and DOANE, J. W., *Phys. Rev. A* **7** (1973) 1366.

[16] LUZ, Z. and MEIBOOM, S., *J. Chem. Phys.* **59** (1973) 275.

[17] BLINC, R., LUZAR, M., VILFAN, M. and BURGAR, M., *J. Chem. Phys.* **63** (1975) 3445.

[18] HERVET, H., DIANOUX, A. J., LECHNER, R. E. and VOLINO, F., *J. Physique* **37** (1976) 587.

[19] LÖSCHE, A. and GRANDE, S., Proceedings 18th Ampere-Congress-Nottingham (1974), 201.

[20] LÖSCHE, A., Int. Summer School, Portoroz, Yugoslavia, 28.6-2.7.1974.

[21] MARTINS, A. F., Thèse Docteur ès Sciences, Grenoble (1972).